Int. J. Electrochem. Sci., 14 **(2019)** 5008 – 5025, doi: 10.20964/2019.06.17

International Journal of
ELECTROCHEMICAL
SCIENCE
www.electrochemsci.org

Corrosion Inhibition of Cold Rolled Steel by Methyl Violet in Phosphoric Acid Containing Chloride Ion

Yan-Ju Yang, Hui Liu, Dong-Mei Lu, Li Peng and Lin Wang[*]

School of Chemical Science and Technology, Key Laboratory of Medicinal Chemistry for Nature Resource, Ministry of Education, Yunnan University, Kunming, Yunnan, 650091, P. R. China;
[*]E-mail: wanglin@ynu.edu.cn (L. Wang); wanglin2812@163.com

Received: 2 February 2019 / *Accepted:* 18 March 2019 / *Published:* 10 May 2019

This paper investigates the inhibition effects of methyl violet (MV) without and with chloride ion on cold rolled steel corrosion in 1.0 mol/dm^3 phosphoric acid (H_3PO_4) solution using weight loss, potentiodynamic polarization and electrochemical impedance spectroscopy techniques. The results reveal that combination of MV and chloride ion shows as excellent inhibitor and there is a stronger synergistic effect between MV and chloride ion for cold rolled steel corrosion in 1.0 mol/dm^3 H_3PO_4. The electrochemical studies reveal that single MV or combination of MV and chloride ion acts as a cathodic type inhibitor and the corrosion reaction is controlled by charge transfer process. Adsorption of MV on the steel surface follows Langmuir adsorption isotherm with chloride ion and Temkin adsorption isotherm without chloride ion, respectively. The thermodynamic and kinetic parameters (ΔG^o_{ads}, ΔH^o_{ads},ΔS^o_{ads}, K_{ads} and E_a) were obtained and discussed. The adsorption of inhibitor molecules on the surface of cold rolled steel contains a mixed physical and chemical adsorption mechanism and the chemisorption is dominant.

Keywords: Corrosion, Cold rolled steel, Acidic solution, Electrochemistry, Methyl violet, Synergistic inhibition.

1. INTRODUCTION

The metals are always susceptible to corrosion by acid solution. Hydrochloric acid and sulphuric acid are widely used in industrial applications, such as acid pickling, removal undesirable rust, acid descaling, oil-well acidizing and acid cleaning [1]. Phosphoric acid, though a moderately strong acid, also exhibits a relatively strong corrosiveness to ferrous or ferrous alloys [2-3]. In the process of phosphorus chemical industry, metallic material equipment is vulnerable to corrosion attack. As an important chemical product, phosphoric acid is also widely used in industries, such as fertilizer production, food industry, electronics industry, acid pickling, descaling and so on. The cold

rolled steel has been one of the most important metals used as constructional material in many industries process because of its low price and excellent mechanical properties [4-5]. Metals are susceptible to corrosion by acid solutions, resulting in economic losses. The use of inhibitors is one of the convenient, economical and effective ways to inhibit corrosion. [6-8]. Most of the efficient inhibitors are organic compounds containing heteroatoms such as nitrogen [6,9-13], sulphur [14-16], oxygen [17-18], π-electrons and aromatic rings [19-20] in their molecules.

Generally speaking, the corrosion inhibition of these compounds is due to the adsorption of the molecules on the metal surface. The inhibitor molecules are bonded to the metal surface by chemical, physical adsorption or complexation [21-22]. Many factors may affect the adsorption of inhibitor molecules, such as the molecule structure, the type of the aggressive environment and nature of metals. Some studies have shown that compounds containing N are more effective in inhibiting corrosion of steel in hydrochloric acid than in sulphuric acid solution, and the possible reason is that there is a synergistic effect between compounds containing N and chloride ions on inhibition of steel corrosion in hydrochloric acid [23-24]. Compared with using a single inhibitor, synergistic effect is an effective technology to improve the efficiency of inhibitors and is often used in practice for its efficiency and economy [25-27].

Methyl violet (MV), an analytical chemical indicator, has nitrogen atoms unshared electron pairs and abundant π-electrons aromatic rings. The inhibition of MV and Cl^- on steel corrosion in sulphuric acid has been studied in a previous work [28]. The results showed that MV and chloride ion exhibited a good synergistic inhibition effect on steel corrosion and the inhibition efficiency reached to 91% even at 10 μmol/dm^3 MV. MV and Br^- also showed good synergistic effect on mild steel corrosion inhibition in phosphoric acid solution [29], but Br^- had adverse effects on the environment and health. This research attempts to investigate the synergistic effect of MV and Cl^- for cold rolled steel corrosion inhibition in H_3PO_4 solution using weight loss, Tafel polarization and electrochemical impedance spectroscope (EIS) techniques. It is expected to get some ideas to guide the composing of inhibitors in reality for H_3PO_4 system.

2. EXPERIMENTAL

2.1. Materials

The cold rolled steel specimens used have a composition of (wt%): 0.05% C, 0.019% S, 0.062% P, 0.021% Si, 0.21% Mn and Fe balance.

All experimental solutions were prepared by bidistilled water and AR grade H_3PO_4 and potassium chloride (KCl) were used. Methyl violet was supplied by Merck Chemicals. Figure 1 shows the chemical structure of MV.

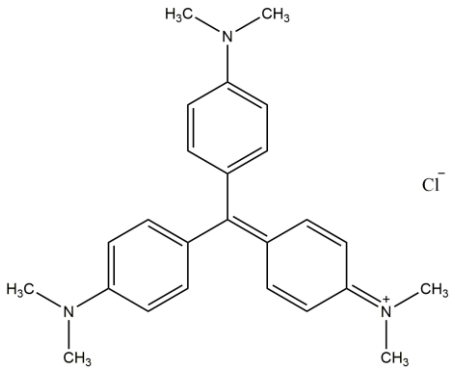

Figure 1. Structure of MV

2.2. Weight loss measurements

The cold rolled steel sheets (40 mm ×15 mm × 0.4 mm) were carefully polished with a series of emery paper grades 600 to 1200 until mirror images were reached. The steel sheets were then cleaned in distilled water, degreased in acetone and dried in airflow.

The steel sheets were accurately weighed and then immersed in the testing solutions (150 ml) for 4 hours. At the end of the run the steel sheets were taken out, washed with distilled water then acetone, dried and immediately weighed accurately. Each measurement was performed on three separate samples and the average weight loss was taken. All runs were done at different concentrations of MV studied without or with 0.1 mol/dm^3 Cl^- in 1.0 mol/dm^3 H_3PO_4 and at 25, 30, 35, 40 ℃.

2.2. Electrochemical measurements

The electrochemical cell consisted of a three-electrode system including a reference electrode, a working electrode and an auxiliary electrode. Saturated calomel electrode (SCE) was used as reference electrode with Luggin capillary positioned very close to the surface of the working electrode in order to minimize ohmic potential drop. Auxiliary electrode was a platinum foil. The working electrodes were cut from a steel plate and were embedded in PVC holder using epoxy resin with an exposed area of 1.0 cm^2. Each working electrode was polished with a series of emery paper grades 600 to 1200 until mirror images were reached, then cleaned in distilled water, degreased in acetone and dried in airflow. Before each measurement, the working electrode was immersed in the 250 ml testing solutions containing different concentrations of MV studied without or with 0.1 mol/dm^3 Cl^- in 1.0 mol/dm^3 H_3PO_4 at open circuit potential (OCP) for two hours until a steady state potential was obtained.

The electrochemical measurements were performed using PARSTAT 2263 Potentiostat/Galvanostat. The Tafel polarization curves were gained on a sweeping range of -250 mV to + 250 mV around OCP, at a sweeping rate of 0.5 mVs^{-1}. EIS measurements were carried out at OCP in the frequency range of 10 mHz -100 kHz using a 10 mV peak to peak voltage excitation. Each experiment was performed in triplicate to ensure reproducibility at 30℃.

3. RESULTS AND DISCUSSION

3.1. Weight loss measurements

The inhibition efficiency (*IE*) was calculated by the following equation [27]:

$$IE = \frac{V_0 - V_i}{V_0} \times 100 \qquad (1)$$

where V_0 and V_i are the corrosion rates in the absence and presence of the inhibitors, respectively. The corrosion rate curves of cold rolled steel with different concentrations of MV without and with 0.1 mol/dm^3 Cl^- in 1.0 mol/dm^3 H_3PO_4 are shown in Figure 2.

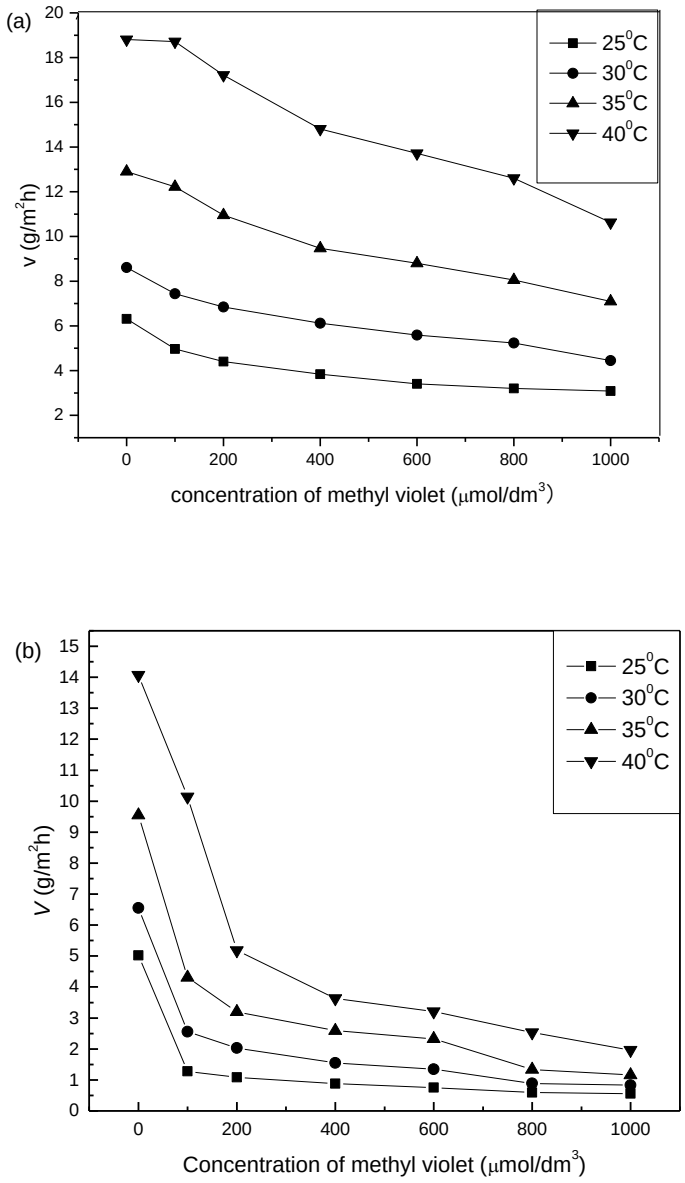

Figure 2. The corrosion rate curves of the cold rolled steel with different concentrations of MV in 1.0 mol/dm^3 H_3PO_4 in the absence (a) and presence (b) of 0.1 mol/dm^3 Cl^-.

According to Figure 2(a), the corrosion rates decrease gradually with increasing MV concentration, but increase with the increase of temperature. Figure 2(b) shows the relationship between MV concentration and corrosion rate in the presence of 0.1 mol/dm^3 Cl^-. Compare Figure 2(a) with Figure 2(b), it is obvious that the corrosion rates greatly reduce with increasing MV concentration with the addition of Cl^- in the experimental temperature range and there are no basically change in corrosion rate values above 800 μmol/dm^3 MV.

Table 1. Inhibition efficiencies for different concentrations of inhibitors in 1.0 mol/dm^3 H_3PO_4 at experimental temperatures.

MV (μmol/dm^3)	Cl^- (mol/dm^3)	Inhibition efficiency			
		25℃	30℃	35℃	40℃
0	0	—	—	—	—
100	0	21	14	5	1
200	0	30	21	15	9
400	0	39	29	27	21
600	0	46	35	32	27
800	0	49	39	38	33
1000	0	51	48	45	43
0	0.1	20	24	27	28
100	0.1	80	70	67	46
200	0.1	83	76	75	72
400	0.1	86	82	81	80
600	0.1	88	84	83	82
800	0.1	91	90	89	86
1000	0.1	91	91	90	89

Table 1 gives the inhibition efficiencies of the cold rolled steel for single MV and combination of MV and Cl^- in 1.0 mol/dm^3 H_3PO_4. As seen, the *IE*s increase gradually with the increase of MV concentration without Cl^-, while the *IE*s decrease with the increase of temperature, which means that the adsorption of MV on the steel surface causes the inhibition of MV on steel corrosion. With the increase of temperature, desorption of MV on the steel surface might be taken place and the cold rolled steel surface will be more exposed to the acidic solution because of reduction of surface coverage of MV on the steel surface [30]. The highest inhibition efficiency is only 51% (at 25℃), and the *IE* of Cl^- alone is also not good.

With the addition of 0.1 mol/dm^3 Cl^- it is clear that the *IE*s have been greatly improved compared with those of MV or Cl^- alone. Such as, the *IE* of the combination of MV and Cl^- exceeds 90% at 800 μmol/dm^3 MV (at 25℃), which also implies that the mixture of MV and Cl^- is an effective corrosion inhibitor for the cold rolled steel in 1.0 mol/dm^3 H_3PO_4 solution.

3.2. Adsorption isotherm

Adsorption isotherms could be commonly used to know the some information on the interaction between inhibitor and steel surface. The following formula can be used to calculate the degree of surface coverage (θ) [27]:

$$\theta = \frac{V_0 - V}{V_0 - V_m} \qquad (2)$$

where V is the corrosion rate in the presence of inhibitor and V_m is the smallest corrosion rate.

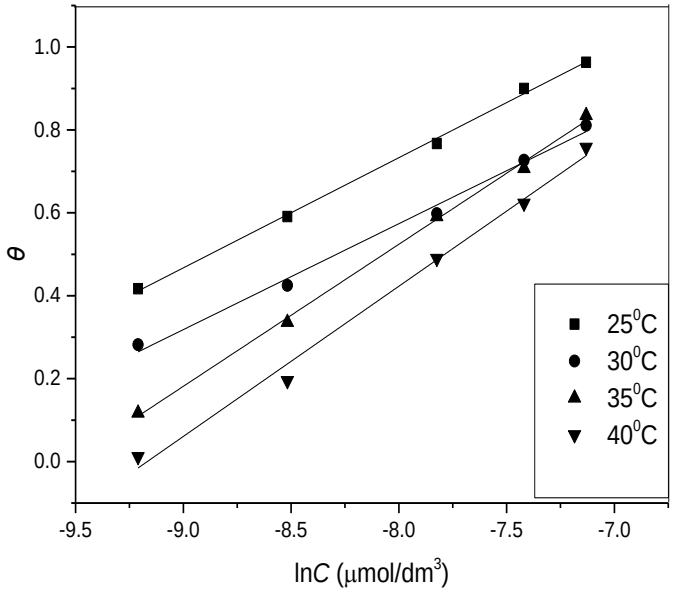

Figure 3. The relationship between θ and ln$C$ in the presence of MV alone in 1.0 mol/dm^3 H_3PO_4.

Table 2. Parameters of the linear regression of θ and ln$C$.

Temperature (℃)	Linear regression coefficient	a	K_{ads} ($\times 10^4$ dm^3/mol)
25	0.9991	-1.88	4.70
30	0.9966	-1.96	2.82
35	0.9990	-1.46	1.38
40	0.9961	-1.38	0.96

It was found that in the presence of MV alone, the adsorption of MV on the steel surface follows the Temkin adsorption isotherm in 1.0 mol/dm^3 H_3PO_4, as follow:

$$\exp(-2a\theta) = K_{ads}C \qquad (3)$$

where C is the concentration of the inhibitor, K_{ads} is the adsorptive equilibrium constant and a is the lateral interaction term describing the molecular interactions in the heterogeneity of the metal surface and the adsorption layer. Equation (3) can also be converted to the following form:

$$\theta = \frac{\ln K_{ads}}{-2a} + \frac{\ln c}{-2a} \qquad (4)$$

Figure 3 exhibits the linear regression of θ and ln$C$ and Table 2 lists the corresponding parameters obtained.

From Table 2, it is clear that the linear regression coefficient values are very close to unity, meaning that the adsorption of MV on the cold rolled steel surface obeys the Temkin adsorption isotherm without Cl^-. The values of K_{ads} are large to 10^4, showing there is stronger adsorption MV onto the steel surface. But it can also be seen that the values of a are < 0, implying that there is a repulsion in the adsorption layer.

In the presence of 0.1 mol/dm^3 Cl^-, the adsorption of MV on the steel surface is fitted to the Langmuir adsorption isotherm:

$$\frac{C}{\theta} = \frac{1}{K_{ads}} + C \qquad (5)$$

Figure 4 gives the relationship of C/θ and C and Table 3 lists the corresponding parameters obtained.

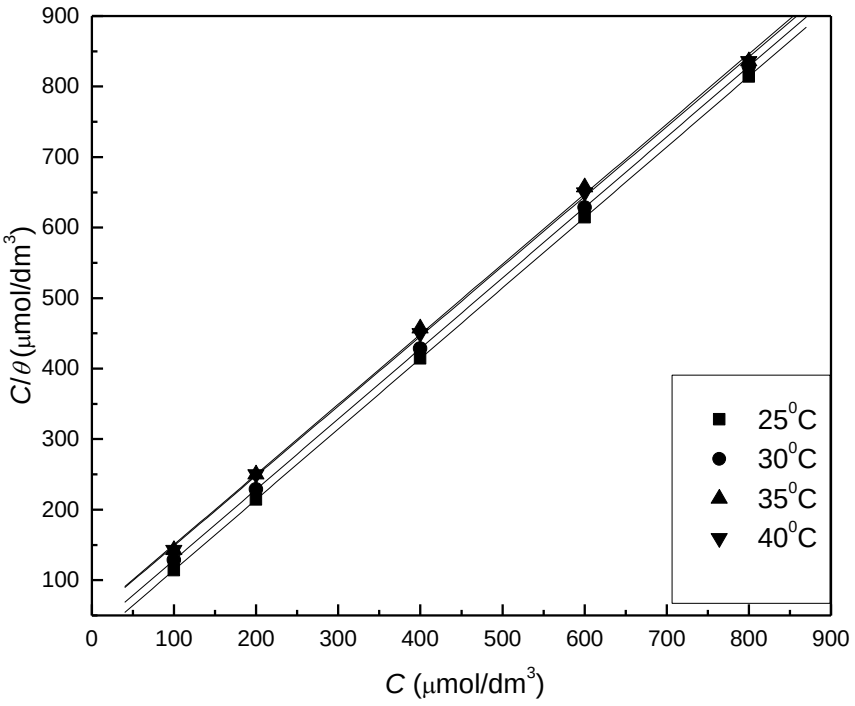

Figure 4. The relationship between C/θ and C in the coexistence of MV and Cl^- (0.1 mol/dm^3) in 1.0 mol/dm^3 H_3PO_4.

Table 3. Parameters of the linear regression of C/θ and C.

Temperature (℃)	Linear regression coefficient	slope	K_{ads} ($\times 10^4 dm^3/mol$)
25	0.9997	0.9879	4.60
30	0.9995	0.9875	2.71
35	0.9976	0.9839	2.05
40	0.9998	0.9723	1.61

Compared the values of K_{ads} in the absence and presence of 0.1 mol/dm^3 Cl^-, it can be seen that the values of K_{ads} are larger in the presence of Cl^- than the absence of Cl^-, which indicates that the adsorption tendency of combination of MV and Cl^- is greater than presence of MV alone.

The corrosion inhibition of cold rolled steel and the adsorption phenomenon of inhibitor can be further elaborated by some thermodynamic parameters. According to the Van't Hoff equation:

$$\ln K_{ads} = \frac{-\Delta H^{\circ}_{ads}}{RT} + B \qquad (6)$$

where ΔH^o_{ads} is the standard adsorption heat, R is the universal gas constant, T is the absolute temperature and B is a constant. Obviously, the ΔH^o_{ads} can be calculated from the slope of the regression.

Table 4. The thermodynamic parameters of adsorption of MV or MV + Cl^- on the surface of cold rolled steel in 1.0 mol/dm^3 H_3PO_4at experimental temperatures.

Temperature (℃)	Cl^- (mol/dm^3)	ΔG^o_{ads} (kJ/mol)	ΔH^o_{ads} (kJ/mol)	ΔS^o_{ads} (J/mol K)
25	0	-37	-85	-161
30	0	-36	-85	-162
35	0	-35	-85	-162
40	0	-34	-85	-163
25	0.1	-37	-49	-40
30	0.1	-36	-49	-43
35	0.1	-36	-49	-42
40	0.1	-35	-49	-45

The standard adsorption free energy (ΔG^o_{ads}) can also be obtained by the following calculation [31-32]:

$$K_{ads} = \frac{1}{55.5}\exp(\frac{-\Delta G^{\circ}_{ads}}{RT}) \qquad (7)$$

where the value 55.5 is the concentration of water in solution represented in mol/dm^3. The standard adsorption entropy (ΔS^o_{ads}) can be calculated by the basic thermodynamic equation:

$\Delta G^o_{ads}=\Delta H^o_{ads}-T\Delta S^o_{ads}$ (8)

The thermodynamic parameters calculated are listed in Table 4.

It is known that the values of ΔG^o_{ads} around -20 kJ/mol or less negative are assigned for the electrostatic interactions exist between inhibitor and the charged metal surface (physisorption). While those around -40 kJ/mol or more negative are associated with chemisorption as a result of sharing or transferring of electrons from the inhibitor molecules to the metal surface to form a coordinate type of metal bond [33-34].

Whether chloride ion exists or not in 1.0 mol/dm^3 H_3PO_4 solution, the negative values of ΔG^o_{ads} show spontaneous adsorption process of MV on the steel surface. These values of ΔG^o_{ads} suggest that adsorption mechanism of the inhibitor molecules on the cold rolled steel is a combination of both physisorption and chemisorption with emphasis on the latter. The decrease of free energy and inhibition efficiency with the increase of temperature indicates that the adsorption of the inhibitor on the cold rolled steel is not beneficial at higher temperature in H_3PO_4 solution. The physical adsorption could occur through the interaction of electrons on Cl^- or π-bonds in the benzene rings of MV with the active positive centers on metal surfaces, and while the chemical adsorption is the formation of coordinated bond between the d-orbital of iron on steel surface and the inhibitor molecules through one pair electron of N atoms or π-electrons of MV [35-36].

The negative values of ΔH^o_{ads} mean that the adsorption of MV on the cold rolled steel surface is an exothermic process in the absence or presence of Cl^- in 1.0 mol/dm^3 H_3PO_4.The negative entropies show that adsorption is a process of decreasing entropy. Entropy decreases can be attributed to the ordering of inhibitor molecules adsorbed on the steel surface during the adsorption process, which reduces the degree of chaos. Compared with the free movement of inhibitor molecules in solution, the degree of chaos is greater [37].The negative of entropy and negative enthalpy suggests that the exothermic is the driving force of spontaneous process inhibitor molecules adsorbed on the surface of cold rolled steel in 1.0 mol/dm^3 H_3PO_4.

3.3. Effect of temperature

Arrenius formula can be applied to calculate the activation parameters to further elucidate the mechanism of the inhibitors action:

$$\ln V = \frac{-E_a}{RT} + \ln A \qquad (9)$$

where E_a is apparent activation energy and A is pre-exponential factor. Figure 5 shows the Arrenius plots of ln$V$ vs. 1/T.

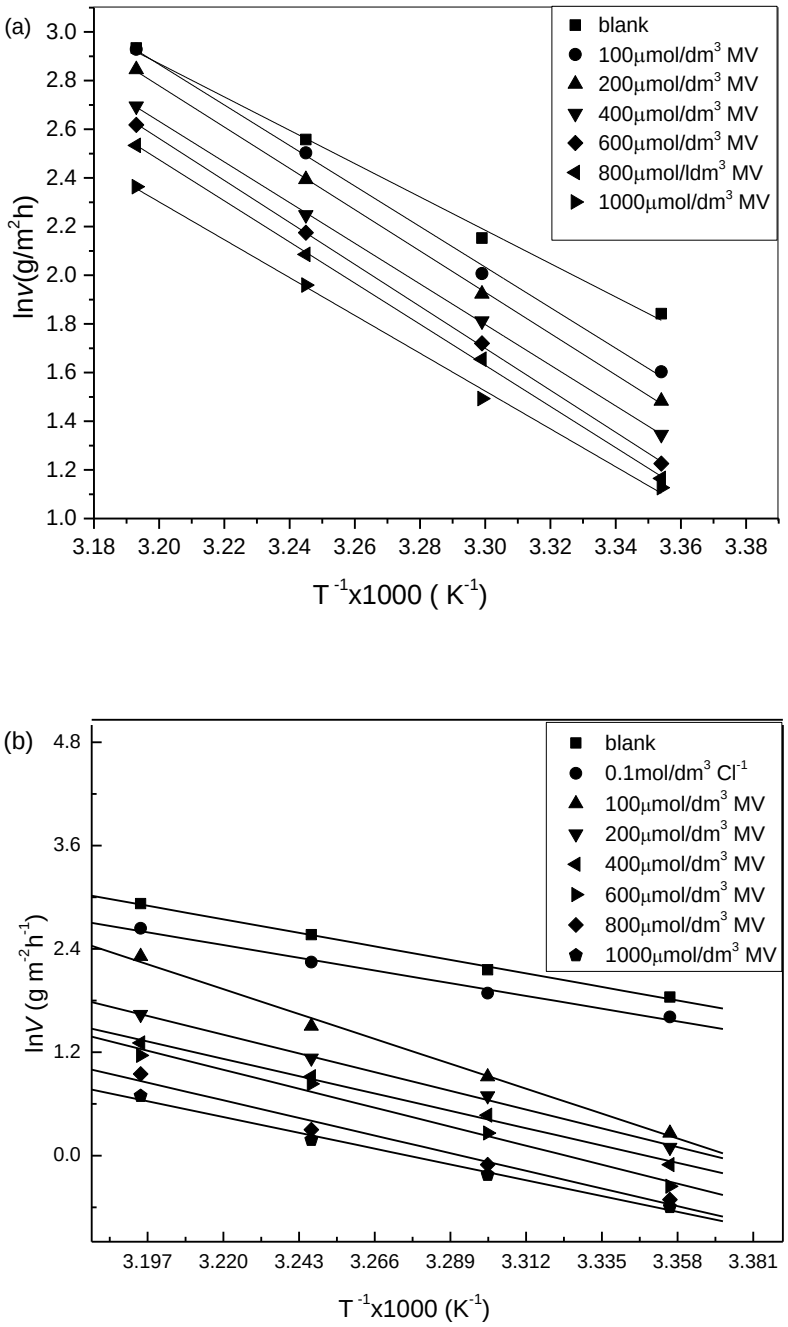

Figure 5. Arrhenius plots of cold rolled steel in 1.0 mol/dm^3 H_3PO_4 without (a) and with (b) 0.1 mol/dm^3 Cl^-.

Table 5 gives the values of E_a and A calculated from the Arrenius formula. It can be found that the values of E_a for inhibited solution were higher than that for the uninhibited solution, which implied the presence of energy barrier on the cold rolled steel surface, meaning that dissolution of the steel in 1.0 mol/dm^3 H_3PO_4 in the presence of MV or combination of MV and Cl^- is lower than the solution with no inhibitor. The increment of the E_a with the addition of inhibitors is indicative of physisorption

of the inhibitor molecules on the metal surface [38]. Considering the E_a values, MV and Cl^- interact electrostatically with steel surface, which is consistent with the result of adsorption free energy.

Table 5. Parameters of the linear regression of ln*V* and 1/*T*.

MV ($\mu mol/dm^3$)	Cl^- (mol/dm^3)	E_a (kJ/mol)	Pre-exponential factor *A* (g/m^2h)	Linear regression coefficient
0	0	57	5.84×10^{10}	0.9982
100	0	69	6.62×10^{12}	0.9991
200	0	70	1.01×10^{13}	0.9998
400	0	69	5.66×10^{12}	0.9999
600	0	72	1.26×10^{13}	0.9992
800	0	69	6.60×10^{12}	0.9998
1000	0	65	6.38×10^{11}	0.9988
0	0.1	53	9.94×10^{9}	0.9941
100	0.1	104	2.52×10^{18}	0.9961
200	0.1	79	9.45×10^{13}	0.9982
400	0.1	73	6.88×10^{12}	0.9965
600	0.1	75	1.13×10^{13}	0.9937
800	0.1	71	1.58×10^{12}	0.9865
1000	0.1	62	4.20×10^{11}	0.9912

It is also clear that the rate of steel corrosion is decided by the E_a and *A* at a certain temperature by equation 9. In the absence or presence of Cl^-, the reduction of corrosion rate of cold rolled steel is all mainly controlled by the increasing the E_a.

3.4. Polarization measurements

Figure 2 gives the potentiodynamic polarization curves of cold rolled steel in 1.0 mol/dm^3 H_3PO_4 at 30℃ for different concentrations of MV without and with 0.1 mol/dm^3 Cl^-.

By Figure 6 (a), MV slightly shifted the corrosion potential (E_{corr}) in the negative direction and slightly promote the anodic reaction, but cathodic polarization was clear in the absence of Cl^-. From Figure 6 (b), combination of MV and Cl^- also slightly shifted E_{corr} to negative direction and retardation of the cathodic reaction was the absolute dominance in the presence of 0.1 mol/dm^3 Cl^-. Compare Figure 6(b) with Figure 6(a), the shifting levels were obviously greater combination of MV and Cl^- than MV alone. These results indicate that the MV alone or combination of MV and Cl^- acted as a cathodic inhibitor for cold rolled steel corrosion in H_3PO_4.

The *IE* values were calculated by the formula [39]:

$$IE = \frac{i_{corr}^0 - i_{corr}^{inh}}{i_{corr}^0} \times 100 \qquad (10)$$

where i^0_{corr} and i^{inh}_{corr} are the corrosion current density values without and with inhibitors, respectively.

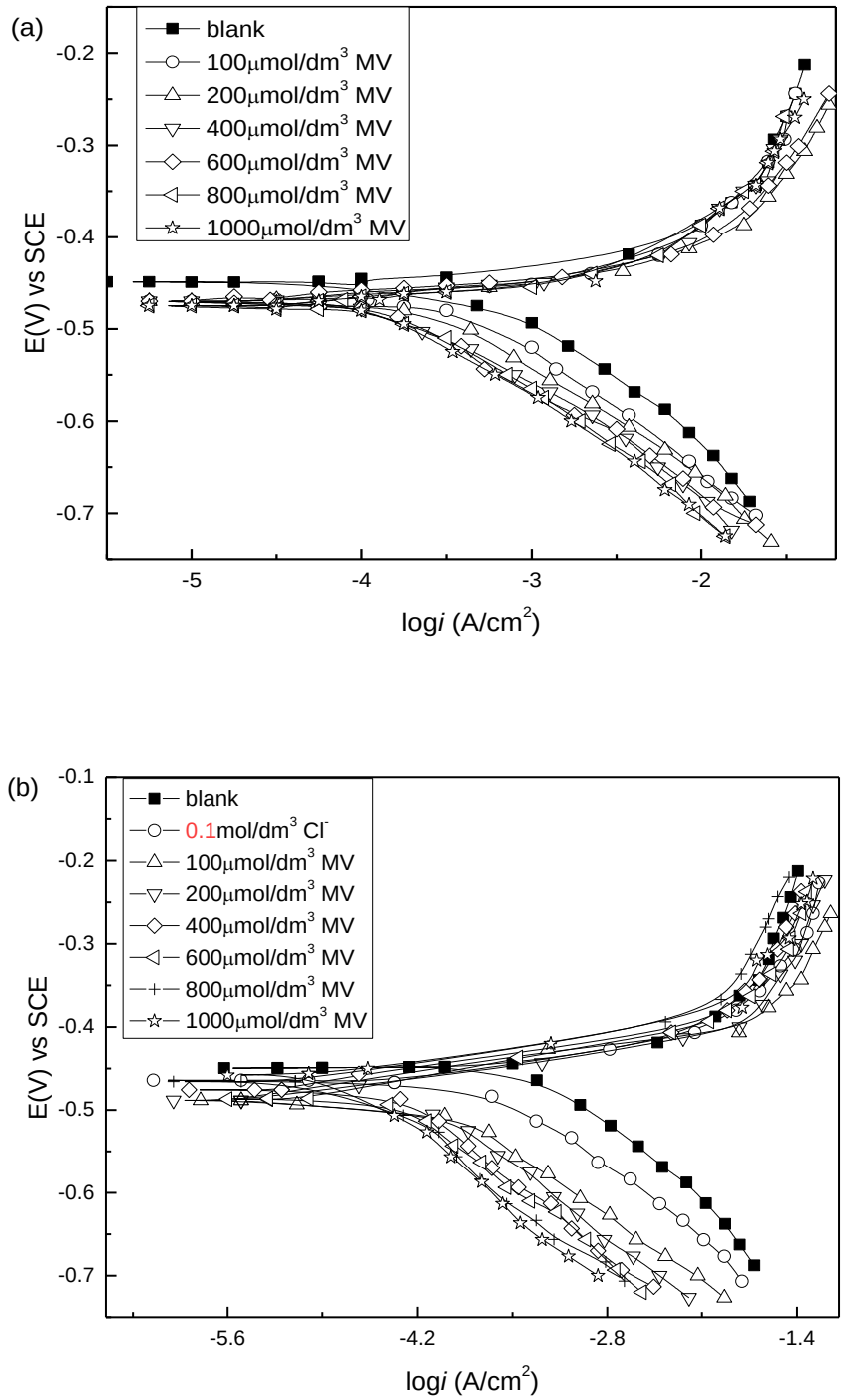

Figure 6. The potentiodynamic polarization curves of cold rolled steel in 1.0 mol/dm^3 H_3PO_4 at 30°C for different concentrations of MV without (a) and with (b) 0.1 mol/dm^3 Cl^-.

Table 6 illustrates corrosion potential (E_{corr}), anodic and cathodic Tafel slopes (β_a, β_c), corrosion current density (i_{corr}) and the inhibition efficiencies for the cold rolled steel corrosion by MV in the absence and presence Cl^- in 1.0 mol/dm^3 H_3PO_4. As seen, Tafel slopes of β_c and β_a do not change regularly and remarkably with the addition of MV or MV and Cl^-, meaning that the cathodic hydrogen evolution was inhibited by the inhibitors through merely blocking the reaction active centers of steel surface without changing the reaction mechanism [40].

Comparing with the inhibition efficiencies, the *IE*s of combination of MV and Cl^- are much greater than those of single MV and the highest *IE* is up to 93% at 1000 μmol/dm^3 MV and 0.1 mol/dm^3 Cl^-, showing that the combination of MV and Cl^- is effective inhibitor for the cold rolled steel corrosion in 1.0 mol/dm^3 H_3PO_4.

Table 6. Polarization parameters for cold rolled steel corrosion containing inhibitors in 1.0 mol/dm^3 H_3PO_4 at 30℃.

MV (μmol/dm^3)	Cl^- (mol/dm^3)	E_{corr} (vs. SCE) （mV）	i_{corr} （μA/cm^2）	- β_c （mV/dec）	β_a （mV/dec）	*IE*
0	0	-449	479	129	38	——
100	0	-473	389	119	39	19
200	0	-477	340	124	56	29
400	0	-478	296	140	67	38
600	0	-482	267	129	70	44
800	0	-482	255	131	47	47
1000	0	-484	239	129	49	50
0	0.1	-464	326	140	49	32
100	0.1	-484	107	120	41	78
200	0.1	-488	88.3	129	44	82
400	0.1	-476	72.3	139	40	85
600	0.1	-487	53.1	136	49	89
800	0.1	-466	42.2	150	42	91
1000	0.1	-458	35.0	148	47	93

3.5. Electrochemical impedance spectroscopy

Nyquist plots for cold rolled steel at 30℃are presented in Figure 7. It is obvious that only a single capacitive loop depressed semicircles is observed for all the Nyquist impedance plots, which implies that the corrosion process occurs under charge transfer control. The inhibition of steel corrosion was influenced predominantly by charge-transfer process and the existence of inhibitors did not affect the mechanism of steel dissolution [41]. The capacitive loops are imperfect semicircles which can be attributed to the frequency dispersion effect as a result of the roughness and inhomogeneous of the electrode surface [42]. It is also seen that diameters of the capacitance loops are clearly larger with Cl^- than without Cl^-, revealing that Cl^- can effectively improve corrosion inhibition performance of MV.

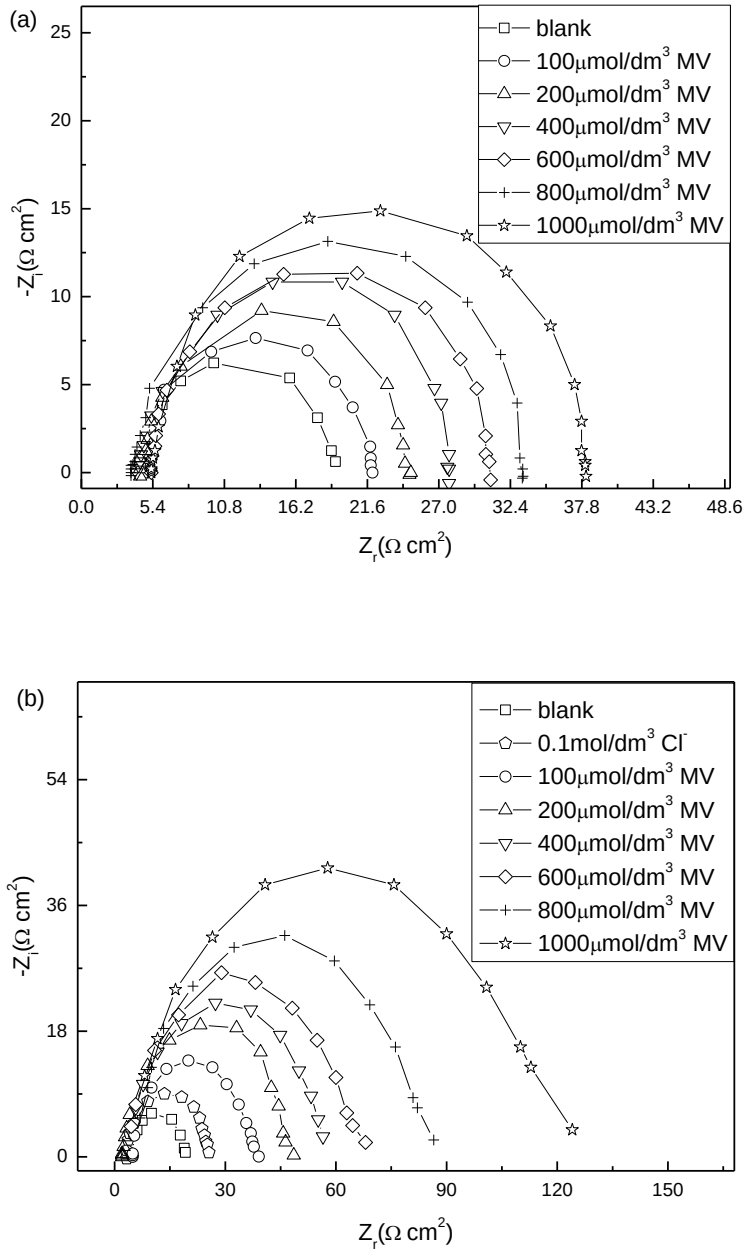

Figure 7. The Nyquist plots for cold rolled steel in 1.0 mol/dm^3 H_3PO_4 at 30°C for different concentrations of MV without (a) and with (b) 0.1 mol/dm^3 Cl^-.

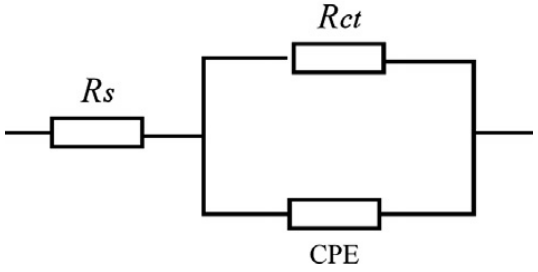

Figure 8. Equivalent circuit used to fit the capacitive loop.

The electrochemical impedance spectroscopy results are simulated according to the equivalent circuit model which is well-known Randle cell, shown in Figure 8, which contains charge transfer resistance (R_{ct}), solution resistance (R_s) and a constant phase element (CPE). The double layer capacitance (C_{dl}) value affected by imperfections of the surface is simulated via CPE [43]. The CPE is composed of a component Q_{dl} and a coefficient α which quantifies different physical phenomena including surface inhomogeneous resulting from surface roughness, porous layer formation, inhibitor adsorption, etc. The C_{dl} can be obtained as follows [24]:

$$C_{dl} = Q_{dl} \cdot (2\pi f_{max})^{\alpha-1} \quad (11)$$

where f_{max} represents the frequency at which the imaginary value reaches a maximum on the Nyquist plot.

The inhibition efficiencies were obtained from the relation:

$$IE_t = \frac{R_{ct(inh)} - R_{ct(0)}}{R_{ct(inh)}} \times 100 \quad (12)$$

where $R_{ct(0)}$ and $R_{ct(inh)}$ are the charge-transfer resistances without and with inhibitor, respectively. The values of EIS parameters are illustrated in Table 7.

Table 7. EIS parameters for cold rolled steel corrosion containing inhibitors in 1.0 mol/dm^3 H_3PO_4 at 30°C.

MV (μmol/dm^3)	Cl^- (mol/dm^3)	R_s (Ω cm^2)	C_{dl} （μF/cm^2）	R_{ct} (Ω cm^2)	IE_{ct}
0	0	4.43	1130	14.6	
100	0	4.85	985	17.4	16
200	0	4.54	935	20.5	29
400	0	4.38	909	23.9	39
600	0	5.01	907	26.1	44
800	0	3.75	756	27.5	47
1000	0	5.18	714	30.3	52
0	0.1	3.31	152	21.6	32
100	0.1	4.43	110	36.8	60
200	0.1	2.53	105	48.6	70
400	0.1	3.88	105	55.2	74
600	0.1`	3.55	102	68.7	79
800	0.1	3.31	95.6	89.4	84
1000	0.1	5.13	75.3	118	88

From Table 7, compared with the blank solution, the capacitance values decrease in the presence of the inhibitor and they show a gradual downward trend with the increase of MV concentration, which means that the decrease of C_{dl} is resulted from the decrease in local dielectric constant or the increase in the thickness of the electrical double layer, suggesting the adsorption of inhibitor molecules at the metal/solution interface [44]. At the same time, It can be observed that R_{ct} and IE_{ct} also increase with the increase of MV concentration, regardless of whether Cl^- exists or not. Of course, this is also obvious that the R_{ct} or IE_{ct} in the presence of Cl^- are much larger than those in

the absence of Cl^-. These results are in good agreement with those obtained from weight loss and polarization measurements.

3.6. Synergism parameters

From the above studies, it is found that the inhibition efficiency for solution with Cl^- exhibit greater values compared to solution without Cl^-. That is to say, the addition of 0.1 mol/dm^3 Cl^- effectively improves the increase of inhibition efficiency comparing with single MV. This means that MV and Cl may have a synergistic inhibition effect on cold rolled steel corrosion in 1.0 mol/dm^3 H_3PO_4 which can be explained by synergism parameters (S), defined as follows [41]:

$$S = \frac{1-(IE_1 + IE_2)}{1-IE_{1+2}} \qquad (13)$$

where IE_1 and IE_2 are the inhibition efficiencies of inhibitor 1 or inhibitor 2, respectively, and IE_{1+2} is the inhibition efficiency by both inhibitor 1 and inhibitor 2.

Generally, when value of *S* is < 1, implying that antagonistic behavior leading to competitive adsorption prevails, whereas *S* > 1 indicates a synergistic effect.

Table 8 gives the values of *S*. Obviously, all S values are greater than 1 and larger, indicating that MV and Cl^- have stronger synergistic inhibition effect on cold rolled steel corrosion and promote the inhibition efficiency to be greatly improved in 1.0 mol/dm^3 H_3PO_4.

Table 8. Synergism parameters of MV and Cl^- on the inhibition of cold Rolled steel corrosion in 1.0 mol/dm^3 H_3PO_4 at experimental temperatures.

MV (μmol/dm^3)	Cl^- (mol/dm^3)	Synergism parameters(*S*)			
		25℃	30℃	35℃	40℃
100	0.1	2.95	2.07	2.06	1.31
200	0.1	2.94	2.29	2.32	2.25
400	0.1	2.93	2.61	2.42	2.55
600	0.1	2.83	2.56	2.41	2.50
800	0.1	3.44	3.70	3.18	2.79
1000	0.1	3.22	3.11	2.80	2.64

In acid solution, steel surface contains positive charge due to E_{corr}–$E_{q=0}$ (zero charge potential) > 0 [45], and MV can also be protonated into $[MVH_x]^{x+}$. Therefore, the adsorption of corrosion inhibitor on steel is first shown as electrostatic action. Due to electrostatic repulsion, it is difficult for positive charged MV to approach the positive charged position on the surface of steel. On the contrary, negatively charged Cl^- is easily adsorbed to the positively charged position of steel surface, resulting in potential of zero charge becomes less negative which promotes the adsorption of inhibitors in cationic form [32,46]. The adsorption of MV can occur through donor-acceptor interactions between the nitrogen atoms or abundance π-electrons of MV and the unoccupied d-orbital of the iron atoms. So, physical and chemical adsorption may be acting on the cold rolled steel surface.

4. CONCLUSION

The corrosion of the cold rolled steel in 1.0 mol/dm^3 H_3PO_4 is not significantly reduced upon the addition of single MV or Cl^-. However, the inhibition efficiency of combination of MV and Cl^- is enormously improved. The synergism parameters indicate that MV and Cl^- show strong synergistic effect for cold rolled steel corrosion inhibition in H_3PO_4. The adsorption of MV on the steel surface follows the Temkin adsorption isotherm without Cl^-. But, the adsorption of MV follows the Langmuir adsorption isotherm with the addition of Cl^-. The adsorption of inhibitor molecules on the steel surface is a spontaneous process with chemical and physical adsorption and chemical adsorption is dominant.

Single MV or combination of MV and Cl^- acts as a cathodic type inhibitor for the cold rolled steel in 1.0 mol/dm^3 H_3PO_4. The inhibitors retard cathodic hydrogen evolution reaction by blocking the active reaction centers on the cold rolled steel surface. EIS shows that the fact the corrosion reaction is controlled by charge transfer.

The results of weight loss, EIS and polarization measurements show good consistency.

ACKNOWLEDGEMENT
This work was financially supported by the National Innovation and Entrepreneurship of College Students Foundation of China(Grant No.201610673001).

References

1. K.C. Emregül and M. Hayvalí, *Corros. Sci.*, 48 (2006) 797.
2. P.B. Mathur, and T. Vasudevan, *Corrosion*, 38 (1982) 171.
3. L. Wang, *Corros. Sci.*,48 (2006) 608.
4. N.S. Ayati, S. Khandandel, M. Momeni, M.H. Moayed, A. Davoodi and M.Rahimizadeh, *Mater. Chem. Phys.*, 126 (2011) 873.
5. G.N. Mu, X.H. Li, Q. Qu, J. Zhou, Acta Chim. Sin. 62 (2004) 2386.
6. G. Sığırcık, D. Yildirim and T. Tüken, *Corros. Sci.*, 120 (2017) 184.
7. D.A. Winkler, *Metals,*7 (2017) 553 doi:10.3390/met7120553.
8. R. Solmaz, G. Kardaş, M. Çulha, B. Yazıcı and M. Erbil, *Electrochim. Acta*., 53 (2008) 5941.
9. S. Ben Aoun, *Int. J. Electrochem. Sci.*, 12 (2017) 10369.
10. L.A. Al Juhaiman, *Int. J. Electrochem. Sci.*, 11 (2016) 2247.
11. G. Sığırcık, T. Tükenand, M. Erbil, *Corros. Sci*., 102 (2016) 437.
12. A.M. Al-Bonayan, *Int. J. Electrochem. Sci.,*10 (2015) 589.
13. A.Y. Musa, A.B. Mohamad, A.A.H. Kadhum and M.S. Takriff, *Int. J. Electrochem. Sci.*, 6 (2011) 2758.
14. M.I. Awad, A.F. Saad, M.R. Shaaban, B.A. AL Jahdaly and O.A. Hazazi, *Int. J. Electrochem .Sci.*, 12 (2017) 1957.
15. G. Žerjav, A. Lanzutti, F. Andreatta, L. Fedrizzi and I. Milošev, *Mater. Corros,* 68 (2017) 30.
16. L. Wang, *Corros. Sci.*, 43 (2001) 2281.
17. M. Mobin, R. Aslam and J. Aslam, *Mater. Chem. Phys.*, 191 (2017) 151.
18. N. M'hiri, D. Veys-Renaux, E. Rocca, I. Ioannoua, N. M. Boudhriouac and M. Ghoul, *Corros. Sci.*, 102 (2016) 55.
19. P. Thanapackiam, S. Rameshkumar, S.S. Subramanian and K. Mallaiya, *Mater Chem. Phys.*, 174 (2016) 129.

20. R. Salghi, D.B. Hmamou, E.E. Ebenso,O. Benali, A. Zarrouk and B. Hammouti, *Int. J. Electrochem. Sci.,*10 (2015) 259.
21. M. Behpour, S.M. Ghoreishi, N. Soltani, M. Salavati-Niasari, M. Hamadanian and A. Gandomi, *Corros. Sci.*, 50 (2008) 2172.
22. G. Quartarone, L. Banaldo and C. Tartato, *Appl. Surf. Sci*., 252 (2006) 8251.
23. R. Fuchs-Godec and M.G. Pavlović, *Corros. Sci.*, 58 (2012) 192.
24. M. Lagrenėe, B. Mernari, M. Bouanis, M. Traisnel and F. Bentiss, *Corros. Sci.*, 44 (2002) 573.
25. A.A. Farag and M.A. Hegazy, *Corros. Sci*., 74 (2013) 168.
26. I.B. Obot, N.O. Obi-Egbedi and S.A. Umoren, *Corros. Sci.*, 51 (2009) 276.
27. L. Wang, S.W. Zhang, Q. Guo, H. Zheng, H.D.M. Lu, L. Peng and J. Xion, *Mater. Corros.*, 66 (2015) 594.
28. L. Wang, F. Yang, J. Ma, Z. Fang, S. Zhang and Q. Guo, *Asian J. Chem.*, 25 (2013) 10305
29. L. Wang, M. Qu, Y. Yang, L. Peng and S. Ma, *Int. J. Electrochem. Sci*., 11 (2016) 9307.
30. E.E. Ebenso and I.B. Obot, *Int. J. Electrochem. Sci*., 5 (2010) 2012.
31. M. Lebrini, M. Lagrenée, H.Vezin, M. Traisnel and F. Bentiss, *Corros. Sci.,*49 (2007) 2254.
32. S.K. Shukla and M.A. Quraishi, *Corros. Sci.*, 51 (2009) 1007.
33. E. Machnikova, K. H. Whitmire and N. Hackerman, *Electrochim. Acta*, 53 (2008) 6024.
34. R. Fuchs-Godec and V. Dlecek, *Collodis Surf.* A., 244 (2004) 73.
35. M.A. Hegazy and M.F. Zaky, *Corros. Sci.*, 52 (2010) 1333.
36. H. Keles, M. Keles, I. Dehri and O. Serindag, *Collodis Surf.* A, 320 (2008) 138.
37. I.B. Obot and N.O. Obi-Egbedi, *Colloids Suf.* A, 330 (2008) 207.
38. E.A. Noor and A.H. Al-Moubaraki, *Mater. Chem. Phys.*, 110 (2008) 145.
39. D. Özkır, K., Kayakırılmaz, E. Bayol, A. Ali Gürten and F. Kandemirli, *Corros. Sci*., 56 (2012) 143.
40. A.K. Satapathy, G. Gunasekaran, S.C. Sahoo, K. Amit and P.V. Rodrigues, *Corros. Sci.*, 51 (2009) 2848.
41. L. Larabi, Y. Harek, M. Traisnel and A. Mansri, *J. Appl. Electrochem.*, 34 (2004)
42. 833.
43. M. Lebrini, M. Lagrenée, M. Traisnel, L. Genembre, H. Vezin and F. Bentiss, *Appl. Surf. Sci.*, 253 (2007) 9267.
44. P. Bommersbach, C. Alemany-Dumont, J.P. Millet and B. Normand, *Electrochim. Acta,* 51 (2006) 4011.
45. M. Behpour, S.M. Ghoreishi, M. Khayatkashani and N. Soltani, *Corros. Sci.*, 53 (2011) 2489.
46. A. Döner, E.A. Şuhin, G. Kardaş and O.Serindağ, *Corros. Sci.*, 66 (2013) 278.
47. H. Ashassi-Sorkabi, N. Gahlebsaz-Jeddi, F. Hashemzadeh and H. Jahani, *Electrochim. Acta,* 51 (2006) 3848.